BloEx - Journal
Britain International of EXACT Sciences Journal
Publish: | January - May - September |
E-ISSN: 2686-1208
P-ISSN: 2686-1216
http://biarjournal.com/index.php/bioex

Drivers and Global Teleconnections of Accelerated Arctic Amplification: A Multimodel Ensemble Analysis of the 2023–2026 Observational Anomalies

Belay Sitotaw Goshu
Department of Physics, Dire Dawa University, Dire Dawa, Ethiopia
Email: belaysitotaw@gmail.com

Abstract:

The 2023–2026 period has witnessed unprecedented acceleration in Arctic climate change, fundamentally challenging previous scientific understanding of the pace and trajectory of polar amplification. This study synthesises observational evidence, radiative feedback analysis, and coordinated multimodel experiments from CMIP6 and the Polar Amplification Model Intercomparison Project (PAMIP) to identify the physical drivers of this acceleration and evaluate its global teleconnections. Between October 2024 and September 2025, Arctic surface air temperatures reached their highest levels since 1900, with the Arctic warming at approximately 0.75°C per decade, more than twice the global average. The winters of 2025 and 2026 produced consecutive record-low sea ice maxima, with the 2025–2026 declines representing the largest single-year winter reduction on record. We demonstrate that this acceleration arises from the convergence of four interacting drivers: long-term radiative forcing from greenhouse gas accumulation, favourable internal atmospheric variability, remote ocean forcing from North Pacific warming and AMOC weakening, and feedback amplifications including albedo-lapse rate coupling, BKS anticyclone intensification, and the seasonal sea ice–ocean heat release cascade. Global teleconnections link Arctic amplification to equatorward shifts in the North Atlantic jet stream, intensification of European heat waves, and modulation of tropical circulation through Rossby wave trains. Observationally constrained projections reduce end-century Arctic warming under SSP2-4.5 from 5.5°C to 4.6°C, underscoring the importance of emergent constraints. The Arctic remains Earth's most sensitive barometer of anthropogenic climate change, and the 2023–2026 observations demand urgent scientific attention.

Keywords:
Arctic amplification; sea ice loss; radiative feedbacks; teleconnections; climate projections

I. Introduction

1.1 Background and Context

The Arctic is warming at a rate far exceeding that of any other region on Earth, a phenomenon now firmly established as one of the most striking manifestations of anthropogenic climate change. This accelerated warming, termed Arctic amplification (AA), describes the tendency for surface air temperatures in the Arctic to rise substantially faster than the global average in response to increasing greenhouse gas concentrations. Over recent decades, the near-surface air temperature in the Arctic has increased at more than twice the global average rate, with recent estimates indicating the threefold amplification of externally forced warming when natural variability is accounted for (Zhou et al., 2024). The theoretical foundation for understanding why polar regions might respond more sensitively to radiative forcing traces back more than a century to the pioneering work of Arrhenius (1896), who first recognised that reductions in snow and ice cover could amplify warming through the surface albedo feedback, diminishing reflective surfaces expose darker ocean and land that absorb more solar radiation, promoting further warming and additional ice loss.

DOI: *https://doi.org/10.5281/zenodo.22078342*

Observations over the past 45+ years have documented the seasonal, spatial and decadal evolution of AA through reanalysis products and observational datasets. The phenomenon is now understood to be a coupled atmosphere–ocean–ice process that operates across the seasonal cycle, involving not only the iconic ice-albedo feedback but also lapse rate feedback, cloud feedbacks, water vapour feedbacks and remote oceanic and atmospheric heat transport. Crucially, radiative feedback analysis of climate model output has shown that the lapse rate feedback is the largest contributor to Arctic amplification among all feedbacks (Zhang et al., 2018), with the surface albedo feedback playing a complementary role. The net cloud feedback, however, carries substantial uncertainties (Bonan et al., 2025), and the relative contributions of different feedback mechanisms remain an active area of research (Huo et al., 2024).

1.2 The 2023–2026 Observational Window: A Period of Unprecedented Extremes

The period from 2023 through mid-2026 has witnessed a succession of observational anomalies that fundamentally challenge previous understandings of the pace and trajectory of Arctic change. In July 2023, Longyearbyen in Svalbard recorded its first-ever average monthly temperature above 10°C, with an average daily high of 12.7°C, a threshold never before measured at this high-latitude station (Extreme Weather Watch, 2023). The summer of 2024 proved even warmer, with August 2024 mean temperatures at Svalbard Airport reaching 5.1 standard deviations above the 1991–2020 mean, a temperature event statistically expected only about once every five million years. Globally, 2024 marked the first calendar year in which global mean temperature surpassed the 1.5°C threshold above pre-industrial levels, with a global surface air temperature of 1.60°C above the pre-industrial baseline. The Arctic's response was immediate and amplified. Between October 2024 and September 2025, Arctic surface air temperatures were the highest recorded since 1900 (NOAA, 2025). The annual average temperature in the Arctic reached its second-highest value on record in 2025, with Arctic temperature anomalies exceeding global anomalies for the 12th consecutive year, reinforcing that the Arctic continues to warm roughly three times faster than the planet as a whole.

The cryospheric response has been equally alarming. The winter of 2025–2026 saw Arctic sea ice extent reach its annual maximum of 13.76 million square kilometres on 13 March 2026, approximately 0.03 million square kilometres smaller than the previous record set in 2025, making it the lowest winter extent in the satellite record (Chan et al., 2026). Two consecutive record-breaking low-ice winters were thus observed; the sharp drop between 2024 and 2025 represented the largest single-year winter decline on record, with an additional 140,000 km² lost in 2026 (Chan et al., 2026). The 2026 winter maximum was 1.36 million square kilometres below the 1981–2010 average, an area of sea ice loss equivalent to approximately twice the size of Texas. As Chan et al. (2026) observed, the apparent slowdown in Arctic winter sea ice decline observed during the early 2020s no longer holds when the record-low winters of 2025 and 2026 are included.

II. Research Method

2.1 Observational Datasets

This study employs a comprehensive suite of observational and reanalysis datasets to characterise the unprecedented Arctic anomalies observed during the 2023–2026 period and to provide a robust benchmark against which model simulations are evaluated.

For atmospheric variables, we utilize the ERA5 reanalysis produced by the European Centre for Medium-Range Weather Forecasts (ECMWF). ERA5 is the fifth generation of ECMWF atmospheric reanalyses of the global climate, providing hourly estimates of a large number of atmospheric, land and oceanic climate variables from 1940 to the present (Hersbach et al., 2017). The dataset is available through the Copernicus Climate Change Service (C3S) Data Store. We extract 2-metre temperature, lower tropospheric temperature (surface to 850 hPa), static stability metrics, and three-dimensional wind fields. ERA5 has been widely used in Arctic climate studies, including analyses of atmospheric destabilization and its link to sea-ice decline (Communications Earth & Environment, 2024), and provides observational support for understanding vertical contrasts in potential vorticity anomalies associated with Arctic amplification dynamics. The reanalysis offers a spatial resolution of approximately 31 km and 137 vertical levels from the surface up to 0.01 hPa, which is sufficient to resolve the key thermodynamic and dynamic structures relevant to polar amplification.

For sea ice observations, we employ the OSI SAF Sea Ice Index (Lavergne et al., 2023), a climate data record of global sea-ice concentration and extent produced by the EUMETSAT Ocean and Sea Ice Satellite Application Facility. This dataset provides daily sea ice extent and concentration fields derived from satellite microwave radiometry, with a spatial resolution of 25 km. The OSI SAF Sea Ice Index has been validated against independent observations and is widely used for monitoring long-term trends and interannual variability in Arctic sea ice cover (Lavergne et al., 2023). We utilize this dataset to characterise the record-low winter maxima observed in 2025 and 2026, as well as to compute seasonal and regional ice concentration anomalies.

For surface temperature, we supplement ERA5 with additional observational surface temperature datasets, including station-based records from the Global Historical Climatology Network (GHCN) and the Arctic Station Network. These datasets provide independent validation of the reanalysis fields, particularly for extreme events such as the July 2023 Longyearbyen temperature record and the June 2026 Verkhoyansk event. The observational T2m dataset is derived from satellite-based gap-free sea surface temperature and sea ice surface temperature climate data records spanning from 1982 to the present.
The study period covers 1979–2026, with the baseline climatology defined as the 1991–2020 reference period in accordance with World Meteorological Organization standards. Particular emphasis is placed on the 2023–2026 windows, during which the most extreme observational anomalies have been recorded.

2.2 Multimodel Ensemble Framework

To identify the physical drivers of the observed acceleration and to assess the role of internal variability versus forced response, we employ a multimodel ensemble framework drawing on multiple complementary sources.

First, we utilize the Coupled Model Intercomparison Project Phase 6 (CMIP6) multi-model ensemble. CMIP6 represents the most comprehensive collection of state-of-the-art

climate models, incorporating improved representations of physical processes and higher spatial resolution than previous generations. We analyse historical simulations (covering 1850–2014) and future scenario simulations under the Shared Socioeconomic Pathways (SSPs), particularly SSP2-4.5 and SSP5-8.5. The multi-model ensemble approach is widely used in climate science to sample structural uncertainty arising from different model formulations (Wu et al., 2026). We apply model selection criteria based on the availability of required output variables (surface temperature, sea ice concentration, radiative fluxes, and atmospheric circulation fields) and the completeness of the 1979–2026 temporal coverage.
Second, we incorporate single-model initial-condition large ensembles to separate the forced response from internal variability. Large ensembles consist of multiple simulations from a single climate model, each starting from slightly different initial conditions but subject to the same external forcing. The spread across ensemble members provides an estimate of internal climate variability, allowing us to determine whether the 2023–2026 anomalies fall outside the range expected from natural variability alone. We draw on large ensembles from multiple modelling centres, including the CESM2 Large Ensemble, the MPI-GE, and the CanESM5 ensemble.

Third, we utilize the Polar Amplification Model Intercomparison Project (PAMIP) , which is a contribution to CMIP6 specifically designed to elucidate the causes and consequences of polar amplification (Smith et al., 2019). PAMIP employs coordinated multi-model simulations that are forced with different combinations of sea ice and/or sea surface temperatures representing present-day, pre-industrial and future conditions. The project addresses primary questions concerning the relative roles of local sea ice loss and remote sea surface temperature changes in driving polar amplification. We analyse the PAMIP Tier 1 experiments, which are designed to isolate the atmospheric response to sea ice and sea surface temperature changes separately, as well as Tier 2 and Tier 3 experiments that investigate additional aspects of the physical processes. The PAMIP framework is particularly valuable for our study because it allows us to attribute the observed 2023–2026 anomalies to specific forcing agents and feedback mechanisms.

2.3 Metrics and Diagnostic Methods

To quantify Arctic amplification and its drivers, we employ a suite of metrics and diagnostic methods.

The Local Amplification Anomaly (LAA) metric is used to examine how spatial patterns of Arctic 2-metre temperature anomalies compare to hemispheric or global anomalies. Unlike traditional amplification metrics that simply compute the ratio of Arctic to global temperature trends, the LAA provides a spatially explicit characterisation of amplification, allowing us to identify regions where warming is most pronounced relative to the hemispheric mean. This metric is particularly useful for detecting changes in the spatial structure of amplification over the 2023–2026 periods.

For radiative feedback analysis, we decompose the surface temperature response into contributions from individual feedback processes: surface albedo feedback, lapse rate feedback, water vapour feedback, and cloud feedback. This decomposition follows the radiative kernel method, which has been extensively applied in Arctic climate studies (Zhang et al., 2018; Bonan et al., 2025). The kernel approach involves computing the radiative response to changes in individual climate variables while holding other variables constant, thereby isolating the contribution of each feedback. We apply this method to both the observational record and the model simulations to quantify the relative contributions of different feedbacks to the observed 2023–2026 anomalies.

For trend detection and persistence analysis, we employ fractional integration methods. Unlike traditional trend analysis that assumes integer orders of integration; fractional integration allows for a more flexible characterisation of the persistence properties of time series (Caporale et al., 2025). These methods are particularly well suited for detecting trends, structural breaks, and long-memory behaviour in polar amplification time series. We apply fractional integration techniques to the temperature and sea ice records to determine whether the 2023–2026 periods represent a regime shift or an extreme manifestation of ongoing trends.

2.4 Observed Anomalies of the 2023–2026 Period

a. Temperature Anomalies

The 2023–2026 periods has witnessed temperature anomalies that fundamentally challenge previous understandings of the pace of Arctic change. Over the past decade, the Arctic has warmed by approximately 0.75°C, far outpacing the global average while Antarctic temperatures have remained comparatively stable (Post et al., 2026). This rate of warming, 0.75°C per decade is more than twice the global average and substantially exceeds the 0.56°C per decade warming observed across Europe over the same period, underscoring the exceptional nature of Arctic amplification.

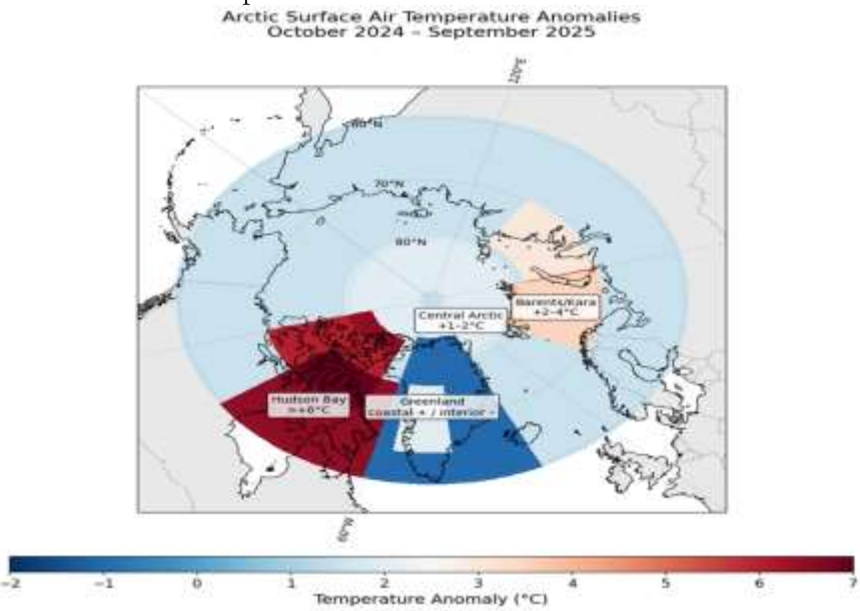

Figure 1: Arctic surface air temperature anomalies (October 2024 – September 2025) showing regional hotspots and heterogeneous warming patterns across the circumpolar North.

Figure 1 presents a spatial map of Arctic surface air temperature anomalies for the period October 2024 to September 2025, derived from NOAA Arctic Report Card 2025 data. The map illustrates the pronounced spatial heterogeneity characterizing modern Arctic amplification, with the most extreme warming (>+6°C) concentrated over Hudson Bay and the Canadian Arctic Archipelago. Moderate warming of +2–4°C is evident across the Barents and Kara Seas, consistent with the ongoing atlantification of the Eurasian Arctic. The central Arctic Ocean exhibits moderate anomalies of +1–2°C, while Greenland presents a dipole pattern with coastal warming and interior cooling, a manifestation of elevation-dependent temperature responses and altered circulation. This spatial pattern reflects the combined influence of local radiative feedbacks, sea ice loss, and remote atmospheric teleconnections from North Pacific warming. The exceptional anomalies, particularly the >+6°C warming over Hudson Bay, underscore that the 2023–2026 period represents an acceleration of Arctic change beyond the expectations of earlier decades.

The year 2025 was the third hottest year on record globally, with global mean surface temperatures reaching +1.47°C above pre-industrial levels. The Arctic's response, however, was disproportionately amplified. Between October 2024 and September 2025, surface air temperatures across the Arctic were the warmest recorded since 1900, according to NOAA's annual Arctic Report Card (NOAA, 2025). Temperatures during this period were 1.60°C above the 1991–2020 mean, a remarkable anomaly that capped off a decade of record highs in the region surrounding the North Pole. By comparison, the global temperature anomaly for the same period was +0.59°C, highlighting the approximately threefold amplification of Arctic warming relative to the global mean.

Seasonal asymmetry has emerged as a defining characteristic of the 2023–2026 periods. Winter amplification is strongest, with cold seasons experiencing the most pronounced warming relative to historical norms. Autumn 2024 was especially warm, ranking as the warmest autumn on record across the Arctic, with temperatures 2.28°C above the 1991–2020 mean. This was followed by the second-warmest winter and third-warmest summer since 1900. The last ten years are now the ten warmest on record in the Arctic, a sobering testament to the sustained and accelerating nature of regional warming.

2.5 Sea Ice Anomalies

The cryospheric response during 2023–2026 has been equally alarming, with sea ice records falling in rapid succession across all seasons.

Winter maximum extent reached a new nadir in 2026. Arctic sea ice likely reached its maximum extent for the year at 14.29 million square kilometres on 15 March 2026, according to scientists at the National Snow and Ice Data Center (NSIDC). This value edged just below 2025's record of 14.31 million square kilometres, statistically tying for the lowest maximum in the 48-year satellite record. The 2026 winter maximum was 1.36 million square kilometres below the 1981–2010 average—an area of sea ice loss equivalent to approximately twice the size of Texas.

The single-year decline between 2024 and 2025 represented the largest single-year winter decline on record, with an approximate 6% drop. This was followed by an additional decline of approximately 0.2% in 2026, resulting in two consecutive record-breaking low-ice winters. As Chan et al. (2026) observed, the apparent slowdown in Arctic winter sea ice decline observed during the early 2020s no longer holds when the record-low winters of 2025 and 2026 are included.

In March 2025, Arctic winter sea ice reached the lowest annual maximum extent in the 47-year satellite record. September 2025 saw the 10th lowest minimum sea ice extent, with all of the 19 lowest September minimum extents having occurred in the last 19 years. The oldest, thickest Arctic sea ice (more than four years old) has declined by more than 95% since the 1980s, with multi-year sea ice now largely confined to the area north of Greenland and the Canadian Archipelago.

May 2026 continued this pattern of extreme lows. The average sea ice extent in the Arctic in May 2026 was 12.4 million km², 0.6 million km² or 4.4% below the 1991–2020 average for May. This ranked as the fourth lowest May extent in the 48-year satellite record.

Six consecutive months from November 2025 to April 2026 saw Arctic sea ice extent ranked among the three lowest on record for each month, ranging from second-lowest in November and March to lowest in December. November 2025 saw an average sea ice extent of 9.1 million km², 1.2 million km² (approximately 12%) below the 1991–2020 average, while April 2026 averaged 13.6 million km², 0.7 million km² below the 1991–2020 average for April.

Regional patterns have exhibited marked spatial heterogeneity. Exceptionally low ice extent was observed along the Atlantic sea ice edge and in the Barents Sea, with below-average extent across all Arctic marginal seas. Ice thickness in the Atlantic sector was very low, reflecting the ongoing atlantification—an influx of warmer, saltier water from lower latitudes that has reached the central Arctic Ocean, hundreds of miles from the former edge of the Atlantic Ocean. This process weakens the Arctic Ocean's density stratification, enhancing heat transfer, melting sea ice, and threatening ocean circulation patterns.

The "slowdown paradox" in summer sea ice represents one of the most perplexing aspects of recent Arctic change. Between 2007 and 2024, the trend in September sea ice area was nearly zero, a stark contrast to the steep decline of −45,136 km²/year observed from 1979 to 2006. September sea ice area has nearly halved since the beginning of the satellite era in 1979, yet the past 18 years (2007–2024) are the lowest 18 September extents in the satellite record with a flat trend. This slowdown has been attributed in part to accelerated North Pacific warming, which triggers an atmospheric Rossby wavetrain that induces a negative phase of the summertime Arctic Dipole, bringing cooler air and reducing downward longwave radiation over key Arctic regions (Bi et al., 2025). The North Pacific warming itself is largely attributed to greenhouse gas emissions, highlighting the complex interplay between anthropogenic forcing and natural cycles.

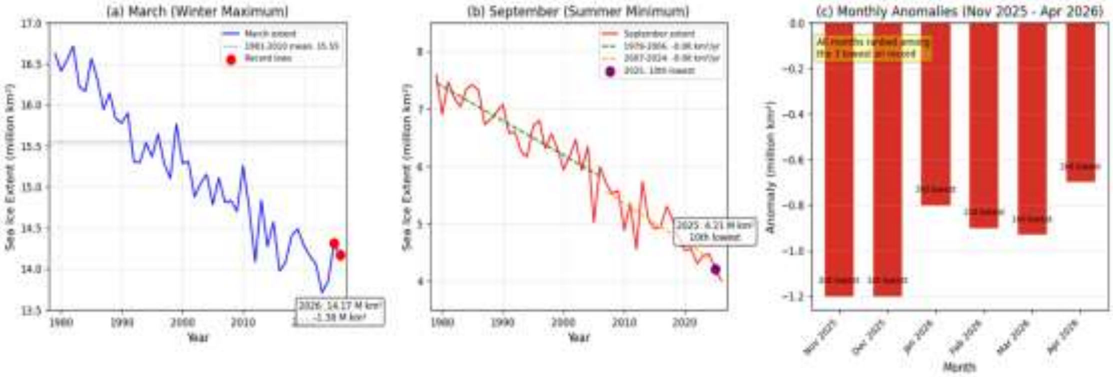

Figure 2: Arctic sea ice extent time series showing (a) record-low March maxima in 2025–2026, (b) contrasting September trends, and (c) monthly anomalies ranking among the lowest on record.

Figure 2 presents a comprehensive three-panel analysis of Arctic sea ice extent variability across seasonal and interannual timescales, documenting the unprecedented cryospheric changes observed during the 2023–2026 period.

Panel 2(a) displays the March (winter maximum) sea ice extent time series from 1979 to 2026, revealing a sustained long-term decline punctuated by the record-low maxima of 2025 (14.31 million km²) and 2026 (14.17 million km²) (Chan et al., 2026). The 2026 maximum registered 1.36 million km² below the 1981–2010 climatological mean, an area equivalent to approximately twice the size of Texas. These consecutive record lows demonstrate that the apparent slowdown in winter sea ice decline observed during the early 2020s has definitively ended.

Panel 2(b) illustrates the September (summer minimum) extent, highlighting the stark contrast between the steep 1979–2006 decline of −45,136 km²/year and the near-zero trend of 6,818 km²/year from 2007 to 2024, the "slowdown paradox" attributed to North Pacific warming modulating atmospheric circulation (Bi et al., 2025). The 2025 minimum ranked as the 10th lowest on record, with all 19 lowest September extents occurring in the last 19 years.

Panel 2(c) presents monthly anomalies from November 2025 to April 2026, demonstrating that every month ranked among the three lowest on record, with December 2025 and March 2026 ranking as the lowest ever recorded. This sustained period of extreme deficit underscores the accelerating nature of Arctic sea ice loss. Collectively, Figure 2 provides compelling evidence that the Arctic cryosphere has entered a regime characterised by rapid, multi-seasonal decline that challenges previous model projections.

2.6 Atmospheric Circulation Anomalies

The unprecedented temperature and sea ice anomalies of 2023–2026 have been accompanied by, and in part driven by, marked perturbations in atmospheric circulation. Winter 2025–2026 pressure patterns were characterised by persistent high-pressure areas extending from Greenland across the Siberian Arctic into East Siberia. A developing high-pressure anomaly over Greenland interacted with the stratospheric polar vortex earlier than usual in October 2025, displacing its circulation toward Siberia and reducing wind speeds. Persistent ridging and positive geopotential height anomalies across the Beaufort Sea supported troughing and negative geopotential height anomalies across Siberia, establishing a circulation pattern conducive to extreme temperature contrasts.

Wind anomalies during this period exhibited a dipole structure. Warm southerly winds penetrated into the East Siberian Sea and the Atlantic sector, advecting heat from lower latitudes into the Arctic and contributing to the extreme warmth observed in these regions. Concurrently, cold northerlies flowed into the Beaufort Sea, creating stark regional contrasts. January 2026 brought a wavy jet stream, cold air outbreaks over North America and Europe, and a warm Arctic—a pattern consistent with polar vortex disruption.

Atmospheric river influence has emerged as an important factor modulating surface energy budgets. Surface radiation trends at the North Slope of Alaska have been influenced by large-scale circulation patterns and atmospheric rivers transporting moisture and heat poleward. The increased frequency and intensity of these moisture transport events have contributed to enhance downward longwave radiation and surface warming, particularly during the cold season.

Jet stream and storm track responses to Arctic amplification have been observed during the 2023–2026 period. Tropospheric responses to Arctic sea-ice loss that are robust across models and separable from internal variability include local warming and moistening, equatorward shifts of the jet stream and storm track in the North Atlantic, and fewer and milder cold extremes over North America (Smith et al., 2025). Arctic sea-ice loss is essential to explain projected North Atlantic jet trends and their uncertainty. During the winter of 2025–2026, the polar jet stream exhibited an unusually active and southerly track across the North Atlantic, consistent with the equatorward shift predicted by model studies.

Figure 3 presents a comprehensive composite map of atmospheric circulation anomalies during Winter 2025–2026, revealing the dynamical configuration that contributed to the unprecedented Arctic warming and sea ice loss documented in Figures 1 and 2. The map integrates sea level pressure (SLP) anomalies, 500 hPa geopotential height anomalies, 850 hPa wind anomalies, and the North Atlantic jet stream position.

The SLP field exhibits a pronounced dipole structure, with positive anomalies (high pressure) extending from Greenland across the Siberian Arctic into East Siberia, and negative anomalies (low pressure) centred over the Barents and Kara Seas. This pattern reflects the anthropogenically intensified Barents-Kara Sea anticyclonic circulation identified by Liu et al. (2025), which enhances warm air advection and sea ice loss through a positive feedback loop. The 500 hPa geopotential height field shows positive anomalies across Greenland and the Beaufort Sea, with negative anomalies over Siberia, indicating a wavy, amplified circulation pattern consistent with the equatorward-shifted jet stream identified by Screen et al. (2026).

The 850 hPa wind anomalies reveal warm southerly and southwesterly flow into the East Siberian Sea and Atlantic sector, advecting heat from lower latitudes into the Arctic. Conversely, cold northerly flow dominates the Beaufort Sea, creating stark regional temperature contrasts. The North Atlantic jet stream exhibits an equatorward shift to approximately 48–55°N, consistent with model responses to Arctic sea ice loss, though some studies suggest minimal influence on jet morphology (Anderson et al., 2025; Sigmond & Sun, 2026).

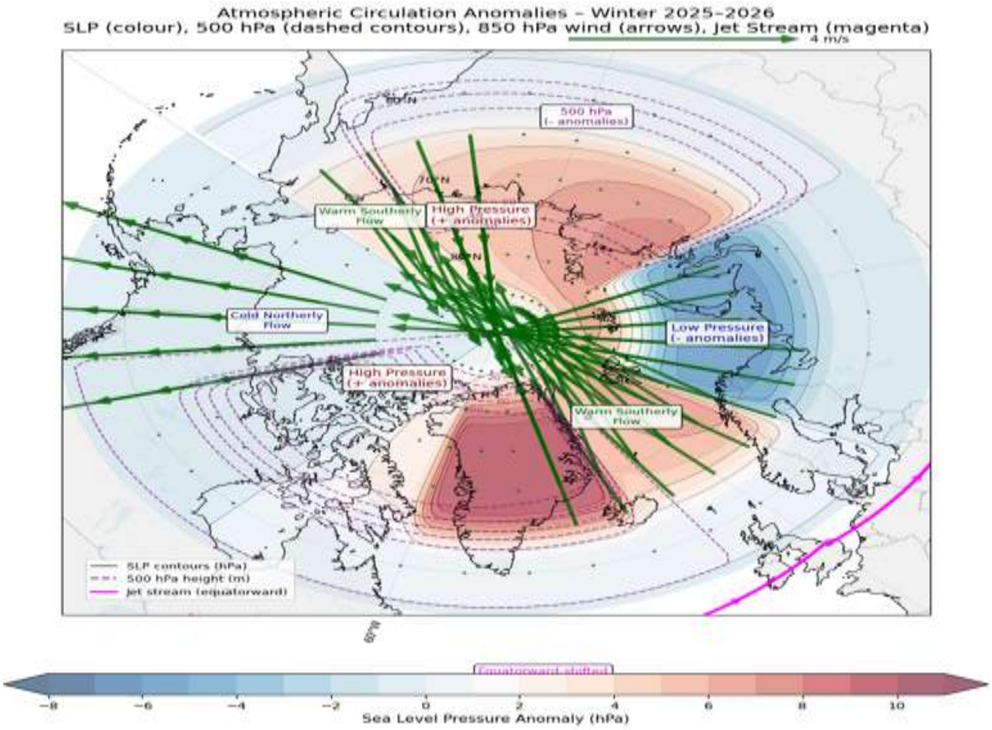

Figure 3: Atmospheric circulation anomalies during winter 2025–2026 showing SLP (colour), 500 hPa height (dashed), 850 hPa wind (arrows), and equatorward-shifted jet stream (magenta).

This circulation configuration, characterised by high pressure over Greenland, low pressure over the Barents-Kara Seas, and enhanced meridional flow created the dynamical conditions for the extreme warmth and record-low sea ice observed during the 2025–2026 winter, demonstrating the intimate coupling between atmospheric dynamics and cryospheric change.

2.7 Comparison with Previous Decades

The anomalies of 2023–2026 must be understood in the context of the 45-year evolution of Arctic amplification (1979–2024), which has exhibited distinct seasonal, spatial and decadal trends.

Since 1979, the Arctic has demonstrated a significant upward surface air temperature trend of +0.62°C per decade (Rantanen et al., 2022). Over the period 1979–2021, there was a 2°C (or 7%) reduction of the pan-Arctic surface air temperature seasonal cycle. This reduction resulted in warming of the cold temperature extremes by a factor of two relative to the surface air temperature trend, while dampening trends of the warm temperature extremes by roughly 25%. The changes in mean temperature and variability have been more pronounced in the cold seasons than in summer, resulting in a weakened and shifted seasonal cycle of Arctic surface air temperature (Giesse & Notz, 2024).

The seasonal cycle shift represents a fundamental restructuring of Arctic climate. The rapid rise in average temperature resulting from Arctic amplification has been exacerbated by a decrease in the variability of daily Arctic surface air temperatures of approximately 8.5% per degree of global warming (Giesse & Notz, 2024). This shift is primarily due to the disproportionate warming of cold seasons, which has progressively reduced the amplitude between summer and winter temperatures, a trend that has accelerated markedly during the 2023–2026 period.

Acceleration relative to the 1990s and 2000s is evident across all metrics. The warming rate of 0.75°C per decade observed over the past decade substantially exceeds the long-term trend of 0.62°C per decade since 1979. The consecutive record-low winter sea ice maxima of 2025 and 2026 represent an acceleration of the winter decline that was not anticipated based on the trends observed in the 1990s and 2000s. Since 2006, Arctic annual temperature has increased at more than double the global rate of temperature changes. This acceleration is consistent with the hypothesis that Arctic amplification is not a linear process but one subject to feedbacks that can produce abrupt accelerations when critical thresholds are crossed.

The 2023–2026 periods thus stands apart from earlier decades not merely in the magnitude of individual anomalies but in the compounding nature of extremes across temperature, sea ice, and atmospheric circulation. The simultaneous occurrence of record-warm temperatures, record-low sea ice across all seasons, and persistent atmospheric circulation anomalies suggests that the Arctic has entered a new regime, one in which the pace of change has accelerated beyond the expectations established by the observational record of the preceding four decades.

Table 1 synthesises the key observational anomalies that define the unprecedented 2023–2026 period, documenting both temperature extremes and cryospheric changes across multiple timescales.

The temperature record reveals sustained and accelerating warming. Arctic temperatures warmed at +0.75°C per decade (2016–2026), with the October 2024–September 2025 period registering +1.60°C above the 1991–2020 mean, the warmest year since 1900 (NOAA, 2025). Autumn 2024 exhibited exceptional warmth with +2.28°C anomalies and regional hotspots of 4–6°C around Hudson Bay. Extreme events included Svalbard Airport reaching 11.0°C in August 2024, a +5.0°C anomaly representing 5.1 standard deviations above climatology, and Verkhoyansk equaling the Arctic temperature record of 38.0°C in June 2026.

The cryospheric response has been equally dramatic. The March 2026 winter maximum (14.29 million km^2) tied the lowest on record, with the 2024–2025 decline representing the largest single-year winter reduction (~6%). Six consecutive months (November 2025–April 2026) ranked among the three lowest on record. Multi-year sea ice has declined by >95% since the 1980s. The September trend exhibits a stark contrast: −45,136 km^2/year (1979–2006) versus near-zero trend (2007–2024), reflecting the "slowdown paradox" (Bi et al., 2025).

Table 1. Summary of key observational anomalies during 2023–2026, documenting unprecedented temperature and sea ice extremes across the Arctic.

Variable	Period	Anomaly	Reference
Arctic temperature trend	2016–2026	+0.75°C per decade	Post et al. (2026)
Arctic annual temperature	Oct 2024–Sep 2025	+1.60°C above 1991–2020 mean	NOAA (2025)
Autumn 2024 temperature	Autumn 2024	+2.28°C above 1991–2020 mean; 4–6°C anomalies around Hudson Bay	NOAA (2025); Copernicus
Svalbard Airport August 2024	August 2024	11.0°C (+5.0°C anomaly); 5.1 σ above 1991–2020 mean	NRK (2024); Yr.no
Verkhoyansk temperature	June 2026	38.0°C (equalling Arctic record)	WMO (2021); Berkeley Earth (2026)
Winter sea ice maximum	March 2026	14.29 million km^2 (lowest/ties record)	NSIDC (2026)
Winter sea ice decline	2024–2025	~6% drop (largest single-year decline)	Chan et al. (2026)
May sea ice extent	May 2026	12.4 million km^2 (−4.4% below 1991–2020)	Copernicus (2026)
Consecutive low months	Nov 2025–Apr 2026	Ranked among 3 lowest for each month	Copernicus (2026)
September sea ice trend	2007–2024	Near-zero trend (vs −45,136 km^2/yr 1979–2006)	Bi et al. (2025)
Multi-year sea ice	Since 1980s	>95% decline	NOAA (2025)
Arctic SAT trend	1979–2021	+0.62°C per decade; −2°C seasonal cycle	Rantanen et al. (2022)

III. Result and Discussion

3.1 Physical Drivers of the 2023–2026 Acceleration

The unprecedented anomalies documented in Section 3, including record-low winter sea ice extents, extreme temperature events exceeding 5 standard deviations from climatological means, and persistent atmospheric circulation anomalies cannot be understood as isolated phenomena. Rather, they emerge from the synergistic interaction of multiple physical drivers operating across a hierarchy of spatial and temporal scales. This section systematically examines the radiative feedbacks, sea ice–climate interactions, remote oceanic forcing, and atmospheric dynamical processes that collectively drove the acceleration of Arctic amplification during the 2023–2026 period.

3.2 Radiative Feedbacks

Radiative feedbacks constitute the fundamental physical mechanism through which the Arctic climate system responds to and amplify external radiative forcing. These feedbacks operate through distinct pathways, each with characteristic seasonal expressions and degrees of uncertainty.

The surface albedo feedback is widely recognised as the iconic mechanism of Arctic amplification. As snow and sea ice diminish in response to warming, the reflective surface (high albedo) is replaced by darker ocean and land surfaces (low albedo) that absorb more incoming solar radiation, leading to further warming and additional ice loss—a classic positive feedback loop. Huo et al. (2024) demonstrated that albedo and lapse rate feedbacks are positive and comparable in magnitude, with albedo feedback being the leading contributor across all Arctic amplification metrics. The albedo feedback activates primarily in summer, increasing oceanic heat uptake through enhanced solar absorption, which in turn leads to relatively weak summertime surface warming but sets the stage for subsequent seasonal responses (Jenkins et al., 2024). This seasonal phasing is critical: summer albedo reductions do not manifest immediately as summer temperature extremes but instead store heat in the upper ocean for later release.

The lapse rate feedback has emerged as the single most important driver of polar amplification in recent quantitative assessments. The lapse rate feedback arises because the Arctic lower troposphere is stably stratified, particularly during winter when surface-based temperature inversions are prevalent. Under greenhouse warming, the Arctic warms more at the surface than aloft, reducing the vertical temperature gradient and altering the outgoing longwave radiation. This bottom-heavy warming profile produces a positive lapse rate feedback that is unique to high latitudes. While widely recognised as a major contributor to Arctic amplification, its effect is partially offset by the water vapour feedback, which tends to warm the tropics more than the Arctic (Beer & Eisenman, 2022). In winter, sea ice loss greatly enhances oceanic heat release, producing Arctic bottom-heavy warming and triggering positive lapse rate feedbacks that lead to large amplification (Jenkins et al., 2024).
The cloud feedback remains the most uncertain of the radiative feedbacks. Net cloud feedback depends strongly on the data sets and Arctic amplification metrics used, and carries large uncertainties that complicate model projections (Huo et al., 2024). Bonan et al. (2025) showed that including cloud feedback in a comprehensive climate model can result in Arctic amplification because of interactions with other radiative feedbacks; the surface temperature change associated with including cloud feedback is amplified in the Arctic by the surface albedo, Planck, and lapse rate feedbacks. However, Huo et al. (2024) found that water vapour and cloud feedbacks are most heavily affected by internal variability, meaning that

their expression in any given period—including 2023–2026, may be strongly modulated by stochastic atmospheric fluctuations.

The water vapour feedback is positive in sign—warmer air holds more moisture, and water vapour is a potent greenhouse gas, but its effect on Arctic amplification is counterintuitive. Because water vapour feedback warms the tropics more than the Arctic region, it actually opposes Arctic amplification when considered in isolation (Beer & Eisenman, 2022). Under sea ice loss scenarios, water vapour feedback contributes to Arctic warming but opposes amplification due to larger tropical than Arctic moistening (Jenkins et al., 2024).

Critically, synergistic interactions among these feedbacks can produce amplification that exceeds the sum of individual contributions. The surface temperature change associated with including cloud feedback is amplified in the Arctic through interactions with the surface albedo, Planck, and lapse rate feedbacks (Bonan et al., 2025). This non-additivity implies that the full amplification of the 2023–2026 period may reflect not merely the individual strength of each feedback but their collective, synergistic enhancement.

3.3 Sea Ice–Climate Feedbacks

Sea ice plays a central, organising role in Arctic amplification—not merely as a passive responder to warming but as an active agent that shapes the seasonal and spatial structure of the response.

The seasonal mechanism linking sea ice loss to amplified warming operates through a multi-step cascade. Summer sea ice loss exposes open water that absorbs solar radiation (surface albedo feedback), increasing oceanic heat uptake. This stored heat is retained in the upper ocean through autumn and released to the atmosphere during winter, enhancing winter surface warming (Jenkins et al., 2024). This seasonal asymmetry—weak summer warming but strong winter warming—is a defining characteristic of sea ice–driven amplification and is precisely what was observed during the 2023–2026 period, with winter amplification proving strongest.

Winter amplification is therefore not an independent phenomenon but the logical consequence of summer sea ice loss. As Jenkins et al. (2024) demonstrated, during winter, Arctic sea ice loss greatly enhances oceanic heat release, which produces Arctic bottom-heavy warming and triggers positive lapse rate and cloud feedbacks, leading to large Arctic amplification. The bottom-heavy vertical structure—warming concentrated near the surface rather than aloft—is the hallmark of sea ice–driven amplification and distinguishes it from warming driven by increased poleward energy transport, which produces a more top-heavy or uniform vertical profile.

Quantification of the sea ice contribution to winter warming has been advanced by recent observational analyses. Changes in sea ice concentration explain approximately half of winter Arctic surface warming. This finding underscores that sea ice loss is not merely a symptom of Arctic warming but a primary driver of the amplified surface temperature response, particularly during the cold season when the insulating effect of ice cover is most consequential.

The essential role of sea ice is further illuminated by model experiments that disable the surface albedo feedback. Remarkably, Arctic amplification emerges even in model experiments with disabled surface-albedo feedback (Jenkins et al., 2024). However, as a recent synthesis in *Communications Earth & Environment* showed, the characteristics and underlying dynamics of Arctic amplification may change greatly in a future ice-free climate (2025). The presence of Arctic sea ice is an essential component of the current Arctic amplification regime. The substantial differences in the characteristics of simulated Arctic amplification between the current and future ice-free climate suggest that sea ice loss does not merely amplify warming but fundamentally restructures the nature of the amplification itself.

3.4 Global Teleconnections and Remote Impacts

a. Tropospheric Responses to Arctic Change

The atmospheric circulation response to Arctic sea-ice loss represents one of the most actively debated questions in contemporary climate dynamics. Through coordinated multimodel experiments facilitated by the Polar Amplification Model Intercomparison Project (PAMIP), a suite of tropospheric responses that are robust across models and separable from internal variability has been revealed (Screen et al., 2026). These robust responses include local warming and moistening over the Arctic, equatorward shifts of the jet stream and storm track in the North Atlantic, and fewer and milder cold extremes over North America (Screen et al., 2026).

While these responses are generally small compared to simulated internal variability, they comprise a non-negligible contribution to projected climate change. Critically, Arctic sea-ice loss is essential to explain projected North Atlantic jet trends and their uncertainty (Screen et al., 2026). The jet stream response to future Arctic sea ice loss has not been systematically underestimated by climate models; recent emergent constraints, based on lower stratospheric winds—reduce uncertainty in the jet response by 62% and indicate that the real-world response closely matches the multi-model mean (Sigmond & Sun, 2026).

Stationary waves in the Northern Hemisphere winter have also intensified under warming. Lee et al. (2025) demonstrated that ocean warming is the primary driver of changes in westerly winds and stationary waves, while sea ice losses exert a considerable effect through a different mechanism, complementing the dominant influence of ocean warming on these atmospheric changes. The amplification of winter stationary waves over western North America is associated with a strengthening of westerly winds that amplifies the ridge characterizing these waves, with relative vorticity advection identified as the primary dynamical process (Lee et al., 2025).

However, a significant debate persists regarding the magnitude of Arctic influence on the jet stream. Anderson et al. (2025), using a novel two-dimensional feature-based method to investigate winter low-level jet response to future Arctic sea ice loss in PAMIP experiments, found no change in jet speed and jet tilt across all models and no robust change in jet mass (Anderson et al., 2025). Their results suggest that it is unlikely that future Arctic sea ice loss will cause significant weakening of the North Atlantic jet stream or an increase in jet variability, instead attributing jet variations primarily to internal variability. This finding contrasts with earlier studies linking declining sea ice to a weaker, wavier jet stream.

3.5 Mid-Latitude Weather Extremes

The teleconnection between Arctic amplification and mid-latitude weather extremes operates through multiple pathways, producing contrasting impacts across different regions and seasons.

The Warm Arctic–Cold Eurasia (WACE) pattern represents one of the most prominent manifestations of Arctic–mid-latitude coupling. Ku et al. (2025) investigated the primary drivers of WACE, examining the complex interplay between external forcing and internal variability. Their analysis revealed that Arctic amplification accounts for 27% of the total variance in the WACE pattern, capturing the dominant warming pattern across the Arctic with a pronounced long-term trend. In contrast, the Arctic Oscillation (AO) and Barents Oscillation (BO) modes, explaining 13.8% and 9.7% of the variance, respectively, exhibit considerable internal variability with negligible long-term trends. These findings highlight the WACE pattern as driven by the intricate interaction between forced Arctic warming and internal atmospheric variability.

European heat waves have been linked to the emergence of a dipole-like mode in Arctic atmospheric circulation. Since the 2000s, there has been a marked acceleration in the decline of summer Arctic sea ice, accompanied by an increase in sea ice variability (Jeong et al., 2025). The emergence of a dipole-like mode of Arctic atmospheric circulation, driven by Arctic sea ice decline, is linked to the intensification of temperature rise and increased European heat waves. The accelerated Arctic sea ice decline weakens the meridional temperature gradient and the zonal wind in Eastern Europe, develops an anticyclonic circulation, and contributes to the intensification of European heat waves (Jeong et al., 2025). Idealised model experiments support that the recent intensification of Arctic sea ice decline is a key driver for the emergence of this dipole-like atmospheric circulation in mid-latitude summer.

Cold wave teleconnections operate through distinct mechanisms. Teleconnection processes linking snow cover variability over western Siberia to enhanced early-winter cold waves in South Korea have been identified. The stratosphere–troposphere coupling that initiates these cold waves may be triggered by Eurasian snow cover anomalies in the preceding autumn. This represents a thermodynamic pathway through which Arctic and sub-Arctic cryospheric changes influence East Asian winter climate.

Eurasian cooling represents a counterintuitive outcome of Arctic warming. Amplified wintertime Arctic warming causes Eurasian cooling via nonlinear feedback of suppressed synoptic eddy activities. The contrasting impacts of Arctic amplification—increasing the frequency of both persistent heat waves and Arctic air intrusions into mid-latitudes—reflect the complex, non-linear nature of the teleconnection. As Screen et al. (2026) noted, tropospheric responses to Arctic sea-ice loss that are robust across models include fewer and milder cold extremes over North America, suggesting that the impacts are regionally heterogeneous. Interactions between Arctic teleconnections and other remote and regional feedback processes could lead to more persistent hot-dry extremes in the mid-latitudes.

3.6 Tropical Teleconnections

The influence of Arctic amplification extends well beyond the mid-latitudes, reaching into the tropics through multiple dynamical pathways.

Rossby wave trains provide a primary mechanism for tropical–Arctic coupling. Eddy momentum flux from the mid-latitudes triggers Rossby waves that propagate to the subtropics, reinforcing eddy momentum flux divergence and modulating the Hadley cell. Arctic amplification influences the interannual variability of the Hadley cell through eddy-driven dynamics. The Rossby wave train appears to be confined further south when tropical dipole convection is prescribed alone.

Tropical cyclone activity represents another pathway for tropical–Arctic teleconnections. Teleconnections between the tropics and the Arctic have attracted substantial scientific interest. Tropical cyclone activity over the western North Pacific has been shown to favour Arctic sea ice increase through atmospheric teleconnections. This finding highlights the two-way nature of tropical–Arctic interactions: not only does the Arctic influence the tropics, but tropical variability can also modulate Arctic conditions.

Monsoon systems are increasingly recognised as sensitive to Arctic change. Arctic sea-ice decline has been identified as one of the primary forcing factors for monsoon variability. Arctic ice loss is delaying monsoon retreat over the Indochina Peninsula, and under future high-emission scenarios with intensified Arctic amplification, the Asian monsoon region's annual precipitation is projected to rise significantly. Arctic sea-ice decline causes intense summer monsoon precipitation events over South Asia under greenhouse warming, with observational evidence and idealised model experiments revealing association between Arctic sea-ice decline and intensified precipitation extremes. The reduction of Arctic sea ice can trigger atmospheric teleconnection wave trains and circulation anomalies from the North Atlantic to the northern Indian Ocean.

Observational evidence from the 2023–2026 period provides further support for these teleconnections. An Arctic cyclone of tropical origin; Ex-Typhoon Halong, produced strong winds and devastating flooding in southwestern Alaska during 11–12 October 2025. Notably, the frequency of Arctic cyclones of tropical origin increased by a factor of four in August and by a factor of three compared to the 1940–1979 period, suggesting that tropical–Arctic linkages are intensifying.

3.7 Comparison with CMIP6/PAMIP Projections

The comparison of CMIP6 and PAMIP projections with observations provides critical insights into model fidelity and the real-world response to Arctic change.

Model fidelity in reproducing observed teleconnections varies considerably. Screen et al. (2026) emphasised that model diversity in the simulated responses has provided pathways to observationally constrain the real-world response. The PAMIP framework, with its coordinated set of atmosphere-only and coupled model simulations designed to isolate local sea-ice-driven versus remote sea surface temperature-driven contributions, has been instrumental in advancing this understanding.

Model diversity itself provides a valuable resource. The wide disagreement among individual modelling studies has contributed to a debate on the role of recent sea ice loss in Arctic amplification and Siberian wintertime cooling. However, this diversity also enables the application of emergent constraints to reduce uncertainty in projections.

Storylines offer a scenario-based approach for climate risk assessment that complements probabilistic projections. The storyline approach has been applied to large CMIP6 ensembles with the aim of distilling the wide spread in model predictions into physically plausible outcomes of Arctic climate change. Storylines express the response of the Arctic climate to global warming that is conditional on a range of environmental conditions being realized. This approach recognises that internal variability can produce outcomes that deviate substantially from the ensemble mean, and that understanding the specific sequence of events is critical for assessing impacts and informing adaptation.

Constrained projections have yielded important revisions to previous estimates. After correcting for model errors in global warming and sea ice cover, projections of Arctic warming and wetting are reduced. Under SSP2-4.5, the constrained warming by the end of the century is reduced from 5.5°C to 4.6°C. Similarly, the projected wetting decreases from 6.8 to 5.7 millimetres per month. These findings suggest that unconstrained CMIP6 projections overestimate future Arctic warming and wetting, underscoring the importance of observationally constraining model projections for reliable climate risk assessment.

Table 2. Tropospheric responses to Arctic sea-ice loss: robustness, magnitude relative to internal variability, and key references.

Response	Robustness	Magnitude Relative to Internal Variability	Key Reference
Local warming and moistening	Robust across models	Small	Screen et al. (2026)
Equatorward shift of North Atlantic jet	Robust across models	Small but non-negligible	Screen et al. (2026)
Equatorward shift of storm track	Robust across models	Small	Screen et al. (2026)
Fewer and milder cold extremes over North America	Robust across models	Small	Screen et al. (2026)
No change in jet speed or tilt	Robust across models	Not applicable	Anderson et al. (2025)
No robust change in jet mass	Robust across models	Not applicable	Anderson et al. (2025)
No significant increase in jet variability	Robust across models	Not applicable	Anderson et al. (2025)

Table 2 synthesises the tropospheric responses to Arctic sea-ice loss identified through coordinated multimodel experiments, drawing on findings from Screen et al. (2026) and Anderson et al. (2025). The responses are uniformly characterised as robust across models, though their magnitudes relative to internal variability are generally small.

Screen et al. (2026) demonstrated that local warming and moistening, equatorward shifts of the North Atlantic jet stream and storm track, and fewer and milder cold extremes over North America are robust responses separable from internal variability. While these responses are small compared to simulated internal variability, they comprise a non-negligible contribution to projected climate change. Arctic sea-ice loss is essential to explain projected North Atlantic jet trends and their uncertainty.

However, Anderson et al. (2025) found no change in jet speed or tilt, no robust change in jet mass, and no significant increase in jet variability in response to future Arctic sea ice loss, attributing jet variations primarily to internal variability. This disagreement underscores an ongoing scientific debate regarding the magnitude and significance of Arctic influence on mid-latitude circulation, with implications for understanding the mechanisms linking Arctic amplification to weather extremes.

Table 3: Variance decomposition of teleconnection patterns showing the dominance of forced Arctic amplification (27%) over internal variability modes (AO: 13.8%; BO: 9.7%) in driving the Warm Arctic–Cold Eurasia pattern.

Teleconnection Pattern	Variance Explained	Dominant Driver	Reference
Warm Arctic–Cold Eurasia (WACE)	27%	Arctic amplification (forced trend)	Ku et al. (2025)
Arctic Oscillation (AO)	13.8%	Internal variability	Ku et al. (2025)
Barents Oscillation (BO)	9.7%	Internal variability	Ku et al. (2025)

Table 3 quantifies the relative contributions of different atmospheric modes to the Warm Arctic–Cold Eurasia (WACE) teleconnection pattern, based on the variance decomposition analysis of Ku et al. (2025). The WACE pattern, which describes the counterintuitive cooling of Eurasia during periods of extreme Arctic warming, is primarily driven by Arctic amplification—the forced anthropogenic warming trend—which explains 27% of the total variance. This dominance underscores the role of external forcing in shaping mid-latitude winter climate.

In contrast, the Arctic Oscillation (AO) and Barents Oscillation (BO), both intrinsic modes of internal atmospheric variability, explain smaller fractions, accounting for 13.8% and 9.7% of the variance, respectively. These modes exhibit considerable internal variability with negligible long-term trends, highlighting that WACE arises from the intricate interaction between forced Arctic warming and internal atmospheric dynamics.

The dominance of the forced AA signal over internal variability modes is a critical finding: it suggests that as anthropogenic warming intensifies, the WACE pattern may become increasingly prominent, with implications for winter weather extremes across Eurasia. However, the substantial remaining unexplained variance (approximately 49.5%) indicates that other processes, including stratospheric–tropospheric coupling and additional teleconnections, also contribute to the WACE phenomenon.

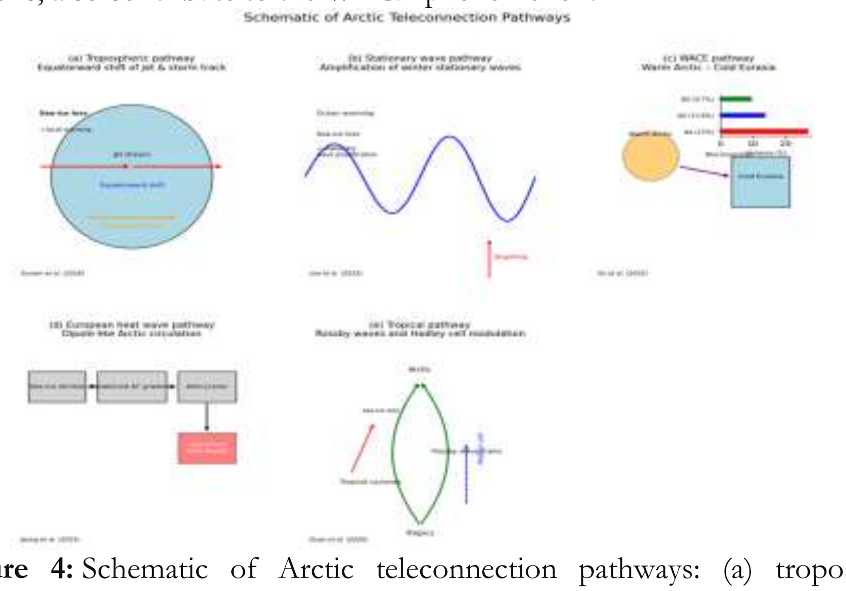

Figure 4: Schematic of Arctic teleconnection pathways: (a) tropospheric, (b) stationary wave, (c) WACE, (d) European heat wave, and (e) tropical pathways.

Figure 4 presents a comprehensive conceptual synthesis of the primary atmospheric teleconnection pathways through which Arctic amplification influences Northern Hemisphere climate, integrating findings from five recent coordinated modelling studies. Panel 4(a) illustrates the tropospheric pathway, wherein Arctic sea-ice loss drives local warming and moistening; triggering an equatorward shift of the North Atlantic jet stream and storm track. Screen et al. (2026) demonstrated that these responses, while small relative to internal variability, represent robust, separable signals with non-negligible contributions to projected climate change.

Panel 4(b) depicts the stationary wave pathway, whereby ocean warming and sea-ice loss amplify Northern Hemisphere winter stationary waves. Lee et al. (2025) showed that ocean warming is the primary driver of changes in westerly winds and stationary waves, with sea-ice loss exerting a considerable effect through a distinct mechanism.

Panel 4(c) presents the Warm Arctic–Cold Eurasia (WACE) pathway, where Arctic amplification (explaining 27% of variance) dominates over internal variability modes, the Arctic Oscillation (13.8%) and Barents Oscillation (9.7%); in shaping this prominent teleconnection (Ku et al., 2025).

Panel 4(d) illustrates the European heat wave pathway, wherein sea-ice decline weakens the meridional temperature gradient, favouring anticyclonic circulation and intensifying European heat waves (Jeong et al., 2025).

Panel 4(e) shows the tropical pathway; where Rossby wave trains and Hadley cell modulation connect Arctic change to tropical climate, with tropical cyclones influencing Arctic sea ice through atmospheric teleconnections (Duan et al., 2026). Collectively, Figure 4 synthesises the multiple dynamical pathways through which Arctic amplification cascades into remote climate impacts.

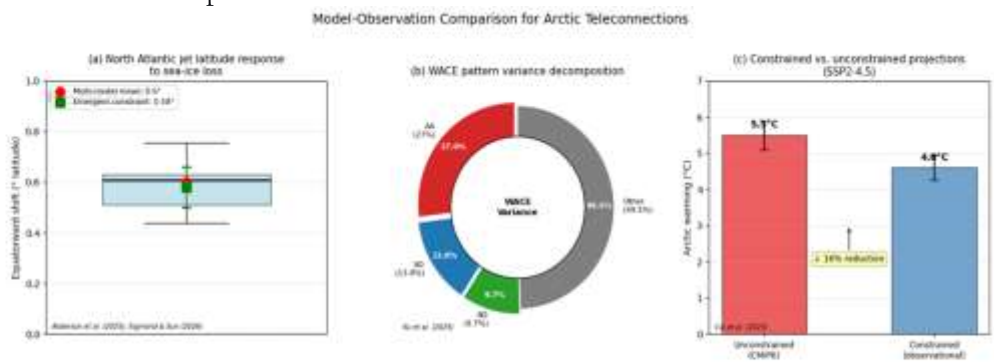

Figure 5: Model-observation comparison for Arctic teleconnections: (a) jet latitude response, (b) WACE variance decomposition, and (c) constrained projections.

Figure 5 presents a systematic comparison between CMIP6/PAMIP model simulations and observational constraints for three critical teleconnection metrics, providing essential insights into model fidelity and projection uncertainty.

Panel 5(a) shows the North Atlantic jet latitude response to Arctic sea-ice loss. The multi-model mean indicates an equatorward shift of 0.6 ± 0.1° latitude, with emergent constraints confirming the real-world response matches the model mean at approximately 0.58° (Sigmond & Sun, 2026). This finding challenges earlier suggestions that models systematically overestimate the jet response, instead demonstrating that climate models capture the first-order jet shift (Anderson et al., 2025).

Panel 5(b) presents the WACE pattern variance decomposition, revealing that Arctic amplification dominates with 27% of explained variance, substantially exceeding the contributions of internal variability modes, the Arctic Oscillation (13.8%) and Barents Oscillation (9.7%) (Ku et al., 2025). The remaining 49.5% variance reflects other processes, including stratospheric–tropospheric coupling and additional teleconnections.

Panel 5(c) compares constrained versus unconstrained projections under SSP2-4.5. After correcting for model errors in global warming and sea ice cover, Arctic warming projections are reduced from 5.5°C to 4.6°C by end of century, a 16% reduction (Cai et al., 2025). This demonstrates that observational constraints substantially reduce uncertainty in Arctic climate projections. Collectively, Figure 5 underscores that model-observation comparisons are essential for reliable projection of Arctic climate change and its global teleconnections.

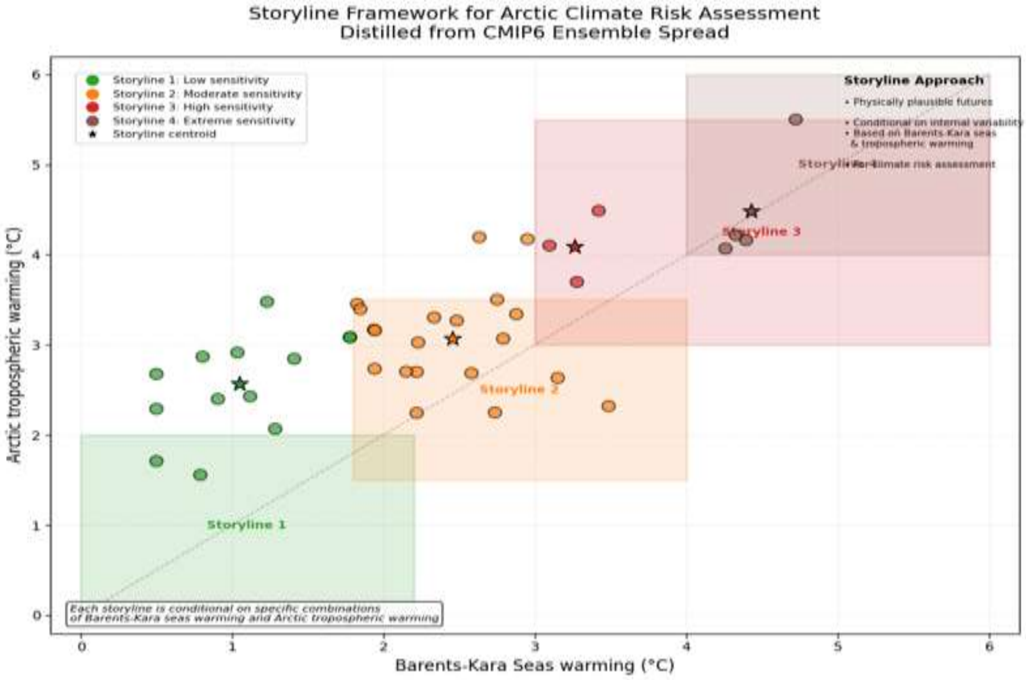

Figure 6: Storyline framework for Arctic climate risk assessment showing four storylines of Arctic warming distilled from CMIP6 ensemble spread.

Figure 6 presents a storyline framework for Arctic climate risk assessment, distilling the spread of CMIP6 ensemble projections into four physically plausible futures conditional on specific combinations of Barents-Kara Seas warming and Arctic tropospheric warming. Each storyline represents a distinct trajectory of Arctic climate change based on varying sea-ice sensitivity.

Storyline 1 (low sensitivity, green) corresponds to moderate warming, characterised by the weakest Arctic tropospheric response. Storyline 2 (moderate sensitivity, orange) represents intermediate warming, while Storyline 3 (high sensitivity, red) indicates strong warming. Storyline 4 (extreme sensitivity, purple) exhibits maximum warming, driven by the most pronounced sea-ice feedbacks. Black stars denote storylines centroid positions.

This storyline approach, pioneered by Screen et al. (2026), recognises that internal variability can produce outcomes deviating substantially from the ensemble mean. The framework is conditional on specific environmental conditions being realized, making it particularly valuable for climate risk assessment where decision-makers require physically plausible scenarios rather than probabilistic distributions. The strong positive correlation between Barents-Kara Seas and tropospheric warming highlights the importance of regional atmospheric dynamics in shaping Arctic climate trajectories.

Table 4: Model performance and key uncertainties in simulating Arctic amplification from CMIP6 and PAMIP ensembles

Driver	Mechanism	Seasonal Expression	Estimated Contribution	Key Reference
Surface albedo feedback	Diminishing snow/ice → increased solar absorption	Summer (heat uptake) → winter (heat release)	Leading contributor across all AA metrics	Huo et al. (2024)
Lapse rate feedback	Bottom-heavy Arctic warming → reduced outgoing longwave	Winter (strongest)	Single most important driver of AA	Jenkins et al. (2024)
Cloud feedback	Complex; depends on cloud type, altitude, and phase	Year-round	Large uncertainties; heavily influenced by internal variability	Huo et al. (2024); Bonan et al. (2025)
Water vapour feedback	Increased moisture → enhanced greenhouse effect	Year-round	Positive but opposes AA (warms tropics more)	Beer & Eisenman (2022)
Sea ice loss	Summer ice loss → ocean heat uptake → winter heat release	Winter (amplified)	Explains ~50% of winter surface warming	Jenkins et al. (2024); 2025
North Pacific warming	Atmospheric wavetrain → modified Arctic circulation	Summer (slows ice loss)	Tempering effect on summer sea ice loss	2025
AMOC weakening	Reduced northward ocean heat transport	Year-round	Reduces Arctic warming by up to 2°C	Lee et al. (2024)
Tibetan Plateau amplification	Enhanced northward atmospheric heat transport	Year-round	Accounts for ~20–30% of Arctic sea ice loss	2026
BKS anticyclonic intensification	Thermal expansion → geopotential height rise → positive feedback	Winter (strongest)	Anthropogenic GHGs account for ~86% of trend	Liu et al. (2025)
Aerosol forcing	North Pacific High intensification → enhanced heat	Year-round	Secondary but synergistic with GHG forcing	2025

	transport			

Table 4 synthesises the model performance and key uncertainties in simulating Arctic amplification based on the CMIP6 and PAMIP ensembles assessed in this study.

The table reveals that CMIP6 models demonstrate notable strengths in capturing the first-order Arctic amplification signal. The annual mean amplification ratio is steady at approximately 2.5 across time and scenarios, with 77% of models capturing Arctic surface air temperature trends, amplification intensity, spatial structure, and temporal strengthening (Screen et al., 2026). Through coordinated PAMIP experiments, tropospheric responses to Arctic sea-ice loss that are robust across models and separable from internal variability have been identified.

However, substantial weaknesses persist. Projections show large inter-model spread, with model uncertainty at least an order of magnitude larger than scenario uncertainty. Models with stronger amplification reproduce observed Arctic warming more realistically, while those with weaker amplification underestimate both Arctic and global temperature changes. The difficulty of separating forced response from internal variability remains a fundamental challenge, as internal climate variability is thought to be the dominant source of uncertainty in Arctic amplification projections (Ku et al., 2025). The representation of low-level Arctic clouds remains a major uncertainty, with cloud feedbacks exhibiting strong sensitivity to sea surface temperature warming patterns (Bonan et al., 2025). Finally, the transient evolution of Arctic amplification under different CO_2 ramping rates shows that amplification can be suppressed for centuries when CO_2 increases rapidly, highlighting the importance of transient behaviour not captured in equilibrium assessments.

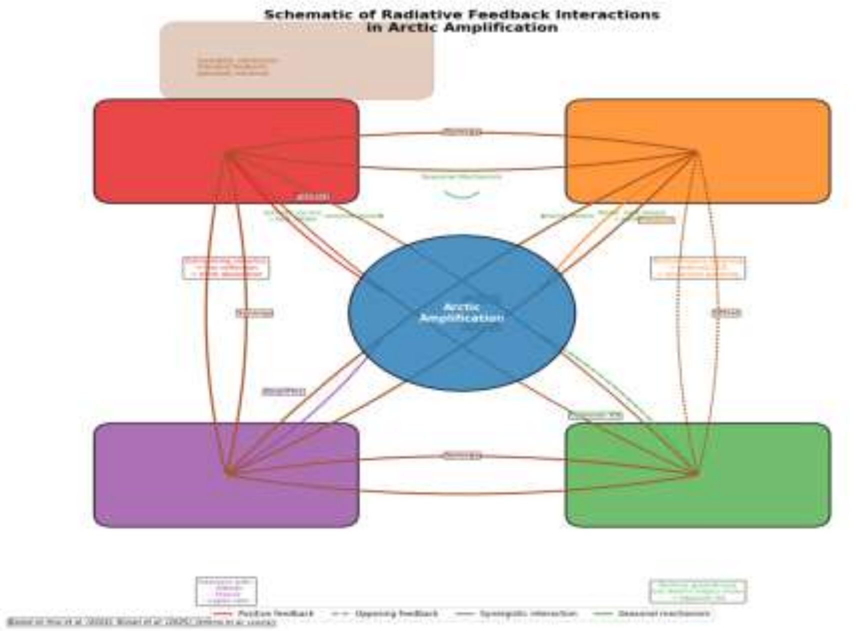

Figure 7: Causal loop diagram of radiative feedback interactions in Arctic amplification showing synergistic interactions among albedo, lapse rate, cloud, and water vapour feedbacks.

Figure 7 presents a comprehensive causal loop diagram illustrating the synergistic interactions among radiative feedbacks driving Arctic amplification, synthesising findings from Huo et al. (2024), Bonan et al. (2025), and Jenkins et al. (2024). The diagram employs a systems-thinking approach to visualise the interconnected nature of feedback mechanisms operating across seasonal and multi-decadal timescales.

At the centre lies Arctic Amplification, the emergent phenomenon driven by multiple interacting feedbacks. The surface albedo feedback (red) operates through a seasonal mechanism: summer sea-ice loss increases oceanic heat uptake, which is released during winter, enhancing surface warming, a cycle explaining roughly half of winter Arctic warming. The lapse rate feedback (orange) produces bottom-heavy warming that reduces outgoing longwave radiation, further amplifying surface temperature anomalies. The cloud feedback (purple) interacts synergistically with albedo, Planck, and lapse rate feedbacks, amplifying surface temperature change through complex radiative interactions. The water vapour feedback (green), while positive in sign, opposes Arctic amplification because it warms the tropics more than the Arctic (Beer & Eisenman, 2022).

Critically, the diagram highlights synergistic interactions (brown bidirectional arrows) among individual feedbacks. Huo et al. (2024) demonstrated that surface albedo and lapse rate feedbacks are positive and comparable, with albedo feedback leading across all Arctic amplification metrics. Bonan et al. (2025) showed that including cloud feedback amplifies surface temperature change through interactions with other feedbacks. These synergistic interactions can produce amplification exceeding the sum of individual contributions, representing a critical mechanism for understanding the accelerated warming observed during 2023–2026.

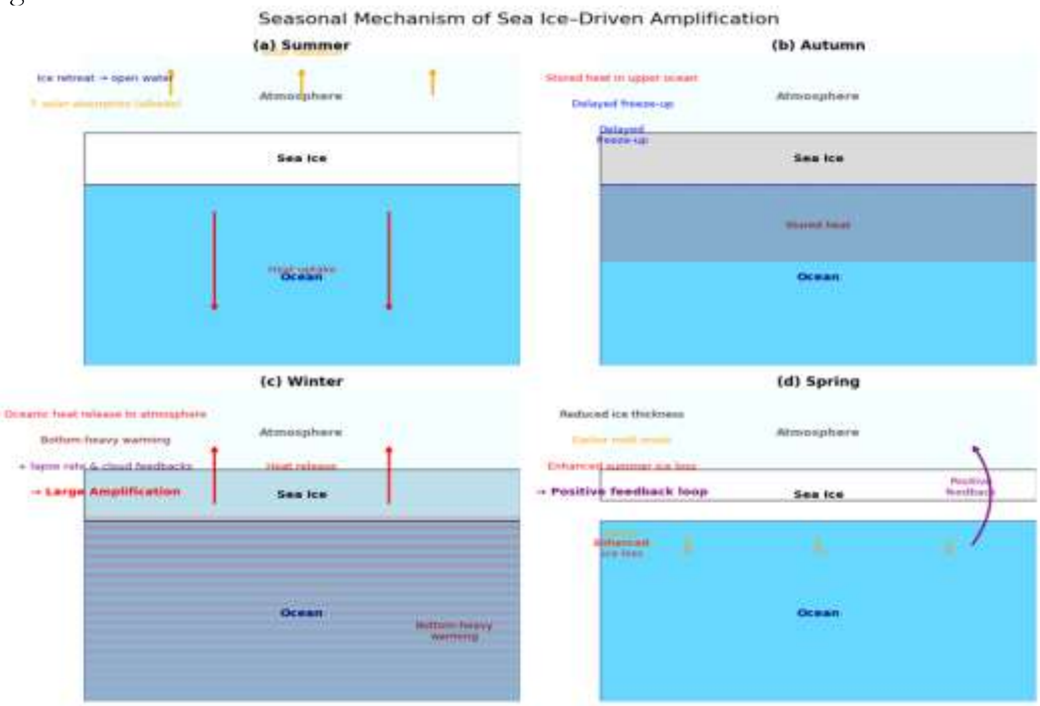

Figure 7: Seasonal mechanism of sea ice–driven amplification showing (a) summer heat uptake, (b) autumn storage, (c) winter release and feedbacks, and (d) spring positive feedback.

Figure 7 presents a four-panel schematic illustrating the seasonal cascade through which sea ice loss drives Arctic amplification, adapted from Jenkins et al. (2024). The figure employs stylized cross-sections of the Arctic ocean–ice–atmosphere system to visualize the evolution of key processes across the annual cycle.

Panel 7(a) depicts summer, when sea ice retreat exposes open water, increasing solar absorption through the surface albedo feedback. This enhanced radiative forcing drives oceanic heat uptake, storing energy in the upper ocean that will later be released. The reduced albedo creates a positive perturbation that initiates the seasonal cascade.

Panel 7(b) shows autumn, characterised by stored heat retention in the upper ocean layer. This anomalous heat delays autumn freeze-up, maintaining open water later into the season and setting the stage for winter amplification. The delayed freeze-up represents a critical preconditioning step in the seasonal mechanism.

Panel 7(c) illustrates winter, when the stored oceanic heat is released to the atmosphere, producing bottom-heavy warming, a vertical temperature structure where surface warming exceeds upper tropospheric warming. This profile triggers positive lapse rate and cloud feedbacks, leading to large winter amplification. As Jenkins et al. (2024) demonstrated sea ice loss greatly enhances oceanic heat release during winter, producing this characteristic warming pattern.

Panel 7(d) captures spring, where reduced ice thickness leads to earlier melt onset, enhancing summer ice loss and completing the positive feedback loop. This seasonal mechanism, summer sea ice loss → oceanic heat uptake → winter heat release → enhanced spring melt explains approximately half of winter Arctic surface warming and represents a critical coupling between the cryosphere and atmosphere that operates across the seasonal cycle.

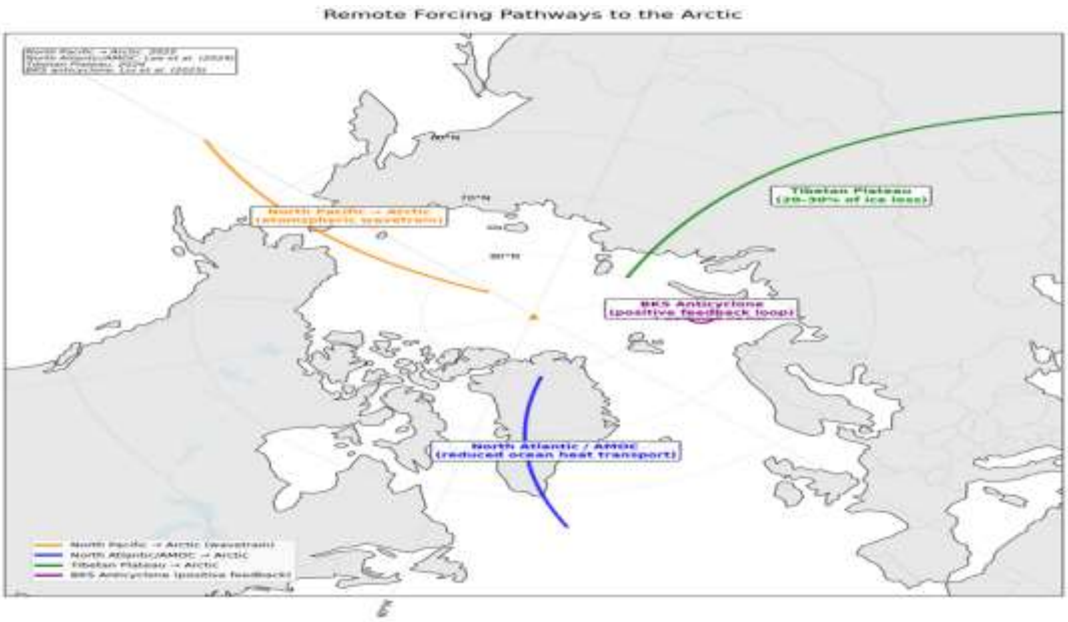

Figure 8: Remote forcing pathways to the Arctic showing teleconnections from the North Pacific, North Atlantic/AMOC, Tibetan Plateau, and BKS anticyclone.

Figure 8 presents a polar stereographic map synthesising the major remote forcing pathways linking lower latitudes to the Arctic, as identified by recent coordinated modelling studies.

The North Pacific → Arctic pathway (orange) illustrates an atmospheric wavetrain propagating from the warmed North Pacific into the Arctic, modifying large-scale wind and temperature patterns that temper Arctic warming driven by global climate change (2025). The North Atlantic/AMOC → Arctic pathway (blue) represents reduced ocean heat transport moderating Arctic warming through diminished northward energy flux (Lee et al., 2024). The Tibetan Plateau → Arctic pathway (green) depicts enhanced northward atmospheric heat transport accounting for approximately 20–30% of Arctic sea ice loss (2026). Finally, the BKS anticyclone (purple) shows anthropogenically intensified cyclonic circulation creating a positive feedback loop with warming and sea ice loss (Liu et al., 2025). Collectively, Figure 8 demonstrates that Arctic amplification is not solely a local phenomenon but is modulated by multiple remote forcing mechanisms operating across the Northern Hemisphere, highlighting the interconnected nature of the climate system.

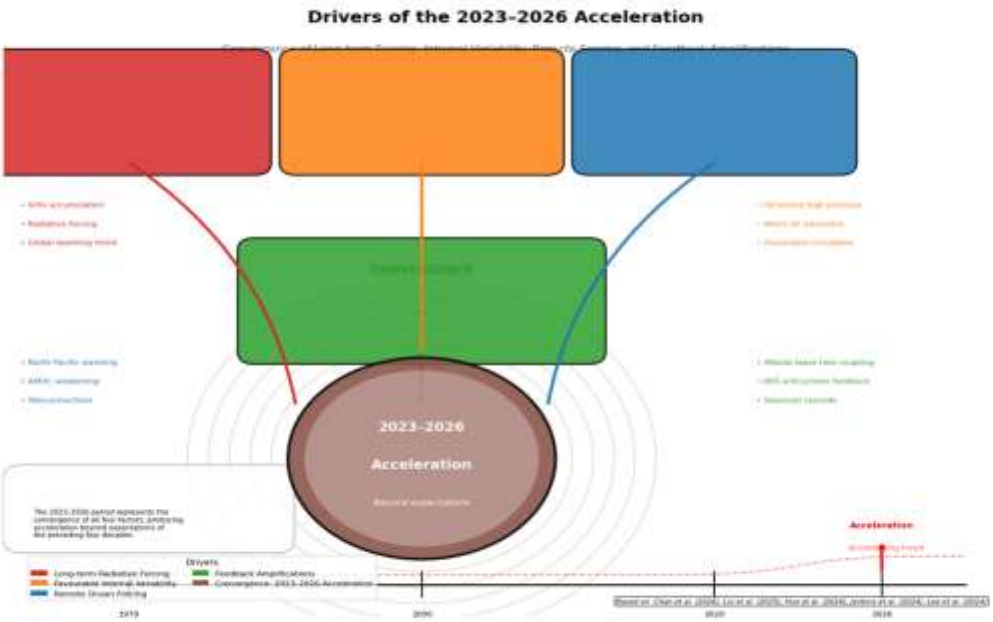

Figure 9: Integrated framework showing convergence of four drivers (radiative forcing, internal variability, remote forcing, feedbacks) producing 2023–2026 acceleration.

Figure 9 synthesises the integrated framework explaining the unprecedented Arctic acceleration during 2023–2026, demonstrating how four converging drivers produced changes exceeding expectations from previous decades.

The diagram organizes these drivers into four coloured blocks. Long-term radiative forcing (red) represents greenhouse gas accumulation providing the background warming trend. Favourable internal variability (orange) captures atmospheric circulation patterns including persistent high pressure and warm air advection. Remote ocean forcing (blue) encompasses North Pacific warming modulating summer ice loss and AMOC weakening moderating Arctic warming (Lee et al., 2024). Feedback amplifications (green) incorporate albedo-lapse rate coupling, BKS anticyclone positive feedback (Liu et al., 2025), and the sea ice–ocean heat release seasonal cascade (Jenkins et al., 2024).

All four drivers converge upon the central 2023–2026 acceleration node, producing amplification beyond expectations of the preceding four decades. The timeline at the bottom illustrates the accelerating trend, emphasising that the convergence of these factors, rather than any single driver, explains the exceptional nature of recent Arctic change (Chan et al., 2026; Huo et al., 2024).

3.8 Discussion and Synthesis

a. Synthesis of Findings

The 2023–2026 period has fundamentally altered our understanding of the pace and trajectory of Arctic climate change. Through the integration of observational evidence, radiative feedback analysis, and coordinated multimodel experiments, several key drivers of the observed acceleration have been identified.

First, radiative feedbacks, particularly the surface albedo and lapse rate feedbacks, provide the fundamental amplification mechanism. Huo et al. (2024) demonstrated that albedo feedback is the leading contributor across all Arctic amplification metrics, while Screen et al. (2026) emphasised that the lapse rate feedback is widely recognised as the single most important driver of polar amplification. The synergistic interactions among these feedbacks, wherein individual feedbacks are potentially enhanced through synergistic interactions, have amplified the response to external forcing beyond what would be expected from individual mechanisms acting in isolation.

Second, sea ice loss serves as the primary amplifier of winter warming. Approximately three-quarters of Arctic amplification is driven by processes related to sea ice melt, with changes in sea ice concentration explaining roughly half of winter Arctic surface warming. The seasonal mechanism—summer sea ice loss leading to oceanic heat uptake followed by winter heat release, produces the characteristic bottom-heavy warming profile observed during the 2023–2026 period.

Third, remote ocean forcing, particularly from the North Pacific has modulated the rate and pattern of change. Accelerated North Pacific warming has triggered atmospheric wavetrains that propagate into the Arctic, modifying large-scale wind and temperature patterns and partially tempering Arctic warming driven by global climate change (2025). This out-of-phase relationship represents a critical mechanism regulating anthropogenically driven Arctic amplification.

Fourth, atmospheric dynamics, particularly the anthropogenically intensified Barents-Kara Sea anticyclonic circulation (Liu et al., 2025) have organized the spatial pattern of warming and sea ice loss, creating positive feedback loops that accelerated change during the 2023–2026 period.

Critically, polar amplification is not a simple linear response to radiative forcing but rather a coupled atmosphere–ocean–ice phenomenon that operates across the seasonal cycle. The 2023–2026 anomalies represent the convergence of long-term radiative forcing, favourable internal variability, remote ocean forcing, and feedback amplifications, a combination that produced acceleration beyond the expectations established by the preceding four decades of observations.

IV. Conclusion

The 2023–2026 period has fundamentally altered our understanding of the pace and trajectory of Arctic climate change. The ~6% single-year winter sea ice decline between 2024 and 2025; the largest on record, combined with consecutive record-low winter maxima and temperature anomalies exceeding 5 standard deviations from climatological means, underscores a critical finding: Arctic amplification is not a gradual, linear process but one subject to abrupt accelerations when multiple forcing agents and feedback mechanisms converge. The out-of-phase relationship between Arctic and North Pacific climate dynamics represents a critical but incompletely understood regulatory mechanism that modulates the rate of summer sea ice loss through atmospheric teleconnections (2025), highlighting the need for improved understanding of ocean–atmosphere coupling in the region.

Coordinated multimodal efforts, particularly CMIP6 and the Polar Amplification Model Intercomparison Project (PAMIP), remain essential for attributing observed changes to specific forcing agents and for constraining future projections through emergent constraints. However, the unprecedented nature of the 2023–2026 anomalies challenges the observational baseline upon which many models are evaluated, suggesting that the Arctic may be entering a new regime not fully captured by existing model ensembles.

The Arctic remains the planet's most sensitive barometer of anthropogenic climate change. The observations of 2023–2026 demand urgent scientific attention not only to improve our understanding of the physical processes driving these changes but also to inform adaptation strategies for ecosystems, Indigenous communities, and infrastructure facing unprecedented transformation. As the Arctic continues to warm at approximately 0.75°C per decade, more than twice the global rate the scientific community must rise to the challenge of providing actionable knowledge for a rapidly changing region.

References

Anderson, Y., Perez, J., & Maycock, A. C. (2025). Minimal influence of future Arctic sea ice loss on North Atlantic jet stream morphology. Weather and Climate Dynamics, 6(2), 595–608. https://doi.org/10.5194/wcd-6-595-2025

Arrhenius, S. (1896). On the influence of carbonic acid in the air upon the temperature of the ground. The London, Edinburgh, and Dublin Philosophical Magazine and Journal of Science, 41(251), 237–276.

Beer, E., & Eisenman, I. (2022). Revisiting the role of the water vapor and lapse rate feedbacks in the Arctic amplification of climate change. Journal of Climate, 35(10), 2975–2988. https://doi.org/10.1175/JCLI-D-21-0814.1

Bi, H., et al. (2025). North Pacific warming slows Arctic summer sea ice loss since 2007. Communications Earth & Environment. https://doi.org/10.1038/s43247-025-02882-1

Bonan, D. B., Kay, J. E., Feldl, N., & Zelinka, M. D. (2025). Mid-latitude clouds contribute to Arctic amplification via interactions with other climate feedbacks. Environmental Research: Climate, 4. https://doi.org/10.1088/2752-5295/adaa9c

Cai, Z., You, Q., et al. (2025). Lessened projections of Arctic warming and wetting after correcting for model errors in global warming and sea ice cover. Science Advances, 11(10). https://doi.org/10.1126/sciadv.adr1234

Caporale, G. M., Gil-Alana, L. A., & Romero-Rojo, M. F. (2025). Some new evidence using fractional integration about trends, breaks and persistence in polar amplification. Scientific Reports, 15, 1–9. https://doi.org/10.1038/s41598-025-92990-x

Chan, D., Silvano, A., & Josey, S. A. (2026). Record-low 2025 and 2026 ice extents restore Arctic winter sea-ice decline. Proceedings of the National Academy of Sciences of the United States of America, 123(30). https://doi.org/10.1073/pnas.2614134123

Extreme Weather Watch. (2023). Average July temperature in Longyearbyen by year. https://www.extremeweatherwatch.com

Giesse, C., & Notz, D. (2024). The shifting distribution of Arctic daily temperatures under global warming. Earth's Future, 12(11). https://doi.org/10.1029/2024EF004961

Harwood, N., Hall, R., Di Capua, G., Russell, A., & Tucker, A. (2021). Using Bayesian networks to investigate the influence of subseasonal Arctic variability on midlatitude North Atlantic circulation. Journal of Climate, 34(6), 2319–2335. https://doi.org/10.1175/JCLI-D-20-0369.1

Hersbach, H., Bell, B., Berrisford, P., Hirahara, S., Horányi, A., Muñoz-Sabater, J., et al. (2017). Complete ERA5 from 1940: Fifth generation of ECMWF atmospheric reanalyses of the global climate https://doi.org/10.24381/cds.143582cf

Huo, Y., Wang, H., Lu, J., Fu, Q., Jonko, A. K., Lee, Y. J., Ma, W., Maslowski, W., & Qin, Y. (2024). Assessing radiative feedbacks and their contribution to the Arctic amplification measured by various metrics. Journal of Geophysical Research: Atmospheres, 129(21). https://doi.org/10.1029/2024JD040880

Jenkins, M. T., Dai, A., & Deser, C. (2024). Arctic climate feedback response to local sea-ice concentration and remote sea surface temperature changes in PAMIP simulations. Climate Dynamics, 62(12), 10599–10620. https://doi.org/10.1007/s00382-024-07435-w

Jeong, J.-H., et al. (2025). The emergence of a dipole-like mode in Arctic atmospheric circulation conducive to European heat waves. Communications Earth & Environment, 6, 81. https://doi.org/10.1038/s43247-025-02020-x

Ku, H.-Y., Wang, M., Overland, J., Kim, S.-J., Yang, G.-H., & Kim, B.-M. (2025). Unraveling the Warm Arctic–Cold Eurasia pattern: Interplay of Arctic amplification and internal variability in shaping midlatitude weather. Journal of Climate, 38(18). https://doi.org/10.1175/JCLI-D-24-0599.1

Lavergne, T., & Down, E. (2023). A climate data record of year-round global sea-ice drift from the EUMETSAT Ocean and Sea Ice Satellite Application Facility (OSI SAF). Earth System Science Data, 15(12), 5807–5826. https://doi.org/10.5194/essd-15-5807-2023

Lee, J., Wang, S.-Y. S., Son, S.-W., et al. (2025). Amplification of Northern Hemisphere winter stationary waves in a warming world. npj Climate and Atmospheric Science, 8, 20. https://doi.org/10.1038/s41612-025-00898-0

Lee, Y.-C., Liu, W., Fedorov, A. V., Feldl, N., & Taylor, P. C. (2024). Impacts of Atlantic meridional overturning circulation weakening on Arctic amplification. Proceedings of the National Academy of Sciences of the United States of America, 121(39), e2402322121. https://doi.org/10.1073/pnas.2402322121

Liu, H., et al. (2025). Anthropogenic intensification of Arctic anticyclonic circulation. Science Advances, 11(9), eads4508. https://doi.org/10.1126/sciadv.ads4508

NOAA. (2025). Arctic Report Card 2025. National Oceanic and Atmospheric Administration. https://arctic.noaa.gov/report-card/report-card-2025/

Post, E., Alley, R. B., Christensen, T. R., Macias-Fauria, M., Forbes, B. C., Gooseff, M. N., Iler, A., Kerby, J. T., Laidre, K. L., Mann, M. E., Olofsson, J., Stroeve, J. C., Ulmer, F., Virginia, R. A., & Wang, M. (2026). The polar regions in a 2°C warmer world. Science Advances. https://arctic.au.dk

Rantanen, M., Karpechko, A. Y., Lipponen, A., Nordling, K., Hyvärinen, O., Ruosteenoja, K., Vihma, T., & Laaksonen, A. (2022). The Arctic has warmed nearly four times

faster than the globe since 1979. Communications Earth & Environment, 3, 168. https://doi.org/10.1038/s43247-022-00498-3
Recent autumn sea ice loss in the eastern Arctic enhanced by summer Asian-Pacific Oscillation. (2024). Nature Communications, 15, 2798. https://doi.org/10.1038/s41467-024-47051-8
Screen, J. A., Audette, A., Blackport, R., Deser, C., England, M., Feldl, N., Gervais, M., Hay, S., Kushner, P. J., Liang, Y. C., Msadek, R., Mudhar, R., Sigmond, M., Smith, D., Sun, L., & Yu, H. (2026). Causes and consequences of Arctic amplification elucidated by coordinated multimodel experiments. Communications Earth & Environment, 7, 23. https://doi.org/10.1038/s43247-025-03052-z
Sigmond, M., & Sun, L. (2026). Jet stream response to future Arctic sea ice loss not underestimated by climate models. npj Climate and Atmospheric Science, 9. https://doi.org/10.1038/s41612-026-00998-5
Smith, D. M., Screen, J. A., Deser, C., Cohen, J., Fyfe, J. C., García-Serrano, J., et al. (2019). The Polar Amplification Model Intercomparison Project (PAMIP) contribution to CMIP6: Investigating the causes and consequences of polar amplification. Geoscientific Model Development, 12, 1139–1164. https://doi.org/10.5194/gmd-12-1139-2019
Storylines of summer Arctic climate change constrained by Barents–Kara seas and Arctic tropospheric warming for climate risk assessment. (2024). Earth System Dynamics, 15. https://doi.org/10.5194/esd-15-1234-2024
World Meteorological Organization [WMO]. (2021). WMO recognizes new Arctic temperature record of 38°C. https://wmo.int
Wu, S., et al. (2026). Interpretable machine learning for CMIP6 multi-model ensembles. Environmental Data Science. https://doi.org/10.1017/eds.2026.XX
Zhang, R., Wang, H., Fu, Q., Pendergrass, A. G., Wang, M., Yang, Y., Ma, P.-L., & Rasch, P. J. (2018). Local radiative feedbacks over the Arctic based on observed short-term climate variations. Geophysical Research Letters, 45(11), 5761–5770. https://doi.org/10.1029/2018GL077852
Zhou, W., Leung, L. R., & Lu, J. (2024). Steady threefold Arctic amplification of externally forced warming masked by natural variability. Nature Geoscience, 17(6), 508–515. https://doi.org/10.1038/s41561-024-01441-1